IJC
International Journal of Cancer

Olfactomedin 4 downregulation is associated with tumor initiation, growth and progression in human prostate cancer

Hongzhen Li[1], Christine Kim[1], Wenli Liu[1], Jianqiong Zhu[1], Kay Chin[1], Jaime Rodriguez-Canales[2,3] and Griffin P. Rodgers[1]

[1]Molecular and Clinical Hematology Branch, National Heart, Lung and Blood Institute, National Institutes of Health, Bethesda, MD
[2]Pathogenetics Unit, Laboratory of Pathology, Center for Cancer Research, National Institutes of Health, Bethesda, MD
[3]Medimmune, Gaithersburg, MD

The olfactomedin 4 (*OLFM4*) gene has been analyzed as a tumor-suppressor gene and a putative biomarker in many cancers. In our study, we analyzed the relationship of *OLFM4* expression with clinicopathological features and with CpG site methylation in the *OLFM4* gene promoter region in human primary prostate adenocarcinoma. OLFM4 protein expression was significantly reduced in prostate cancer tissue compared to adjacent normal tissue and was further significantly reduced in more advanced cancers. Bioinformatic studies with clinical datasets revealed that primary prostate adenocarcinoma patients with reduced OLFM4 mRNA expression exhibited higher Gleason scores and higher preoperative serum prostate-specific antigen levels, as well as lower recurrence-free survival. Three of the eight CpG sites in the *OLFM4* gene promoter region were hypermethylated in cancerous prostate cells compared to adjacent normal cells, and reduced methylation of eight CpG sites was associated with increased OLFM4 mRNA expression in RWPE1 and PC-3 cells. Furthermore, knockdown of *OLFM4* gene expression was associated with enhanced epithelial–mesenchymal transition (EMT)-marker expression in RWPE immortalized normal prostate cells. In contrast, restoration of *OLFM4* expression in PC-3 and DU145 prostate cancer cells lacking *OLFM4* significantly inhibited both EMT-marker expression and tumor cell growth in *in vitro* and *in vivo* models, indicating that OLFM4 may play a tumor-suppressor role in inhibiting the EMT program, as well as tumor initiation and growth, in prostate cells. Taken together, these findings suggest that OLFM4 plays an important tumor-suppressor role in prostate cancer progression and might be useful as a novel candidate biomarker for prostate cancer.

Introduction

Prostate cancer is the most commonly diagnosed solid tumor and the second-leading cause of cancer-related death in American men.[1] Genetics and epigenetic inactivation of tumor-suppressor genes are both involved in the carcinogenesis and progression of all cancers, including prostate.[2] Primary prostate cancers are heterogeneous diseases with variable clinical outcomes. To predict patients' clinical outcomes, histopathological tumor grade (Gleason score), clinical tumor stage and serum prostate-specific antigen (PSA) level have regularly been used for patient care.[3] Recently, primary prostate cancers have been subtyped based on molecular pathologies, which has improved patients' prognoses and allowed the use of personalized therapies.[4] Therefore, efforts to identify additional biomarkers for predicting human prostate cancer progression have been undertaken by many groups worldwide.[5–7]

The epithelial–mesenchymal transition (EMT) plays an important role in the formation of the prostate during

Additional Supporting Information may be found in the online version of this article.

Key words: olfactomedin 4, DNA methylation, prostate cancer, tumor growth, epithelial–mesenchymal transition

Abbreviations: 5-Aza: 5-aza-2′-deoxycytidine; ANOVA: one-way analysis of variance; ATCC: American Type Culture Collection; DMSO: dimethyl sulfoxide; EMT: epithelial–mesenchymal transition; GFP: green fluorescent protein; HE: hematoxylin and eosin; LCM: laser-capture microdissection; OLFM4: olfactomedin 4; PCR: polymerase chain reaction; PSA: prostate-specific antigen; qRT-PCR: quantitative real-time PCR; SD: standard deviation; SDF-1: stromal cell-derived factor-1; SHH: sonic hedgehog; shRNA: short hairpin RNA; TCGA: The Cancer Genome Atlas

Conflict of interest: The authors declare no conflict of interest.

Grant sponsor: Intramural Research Program, National Institutes of Health/National Institute of Diabetes and Digestive and Kidney Diseases

Published 2019. This article is a U.S. Government work and is in the public domain in the USA.
This is an open access article under the terms of the Creative Commons Attribution-NonCommercial-NoDerivs License, which permits use and distribution in any medium, provided the original work is properly cited, the use is non-commercial and no modifications or adaptations are made.

DOI: 10.1002/ijc.32535
History: Received 11 Jan 2019; Accepted 4 Jun 2019; Online 26 Jun 2019

Correspondence to: Griffin P. Rodgers, MD, Molecular and Clinical Hematology Branch, National Heart, Lung, and Blood Institute, National Institutes of Health, Building 10, Room 9N119, 9000 Rockville Pike, Bethesda, MD 20892, USA, Tel.: +1-301-402-2418, Fax: +1-301-480-1940, E-mail: gr5n@nih.gov

What's new?

Altered expression of the *OLFM4* gene appears to be involved in many cancers. In this study of prostate cancers, the authors found that *OLFM4* can suppress tumor initiation, growth and progression. Downregulation of *OLFM4* was associated with higher serum PSA levels, higher Gleason scores, and lower recurrence-free survival in prostate cancer patients. These results indicate that *OLFM4* may play an important tumor-suppressor role in the progression of prostate cancer, and may provide a novel prognostic biomarker for prostate cancer treatment.

development, homeostasis in the adult prostate gland and malignant progression of prostate tumors.[8,9] EMT transcription factors, such as TWIST1, ZEB1 and SNAIL1, have been shown to target the *CDH1* gene and alter E-cadherin expression.[9] It has been reported that TWIST1 is associated with prostate cancer tumorigenesis and chemoresistance, as well as the EMT program in the prostate cancer cell lines PC-3 and DU145.[10] Furthermore, the EMT program is linked to stem-cell-like cells in both mammary glands[11] and prostate cancer.[12]

The olfactomedin 4 (*OLFM4*) gene encodes OLFM4, a secreted glycoprotein belonging to the olfactomedin family.[13] OLFM4 plays important roles in innate immunity, inflammation and cancers.[14] The *OLFM4* gene was first cloned from human myeloid progenitor cells and is normally expressed in prostate, bone marrow, small intestine and pancreas.[13] Altered *OLFM4* gene expression has been observed in prostate cancer, gastrointestinal cancer and myeloid leukemia.[15–17] Furthermore, frequent genetic deletion of the *OLFM4* gene has been reported in advanced prostate cancer and squamous cell carcinoma.[18,19] In addition, DNA methylation of the *OLFM4* gene has been found to be associated with tumor aggressiveness and patient outcomes in gastric carcinoma.[20] The *OLFM4* gene has been analyzed as a putative biomarker in many cancers, including gastrointestinal cancer, head and neck squamous cell carcinoma, cervical neoplasia, nonsmall cell lung cancer, triple-negative breast cancer and distant metastases in estrogen receptor-positive breast carcinoma.[20–32]

In our study, we provide clinical evidence that reduced *OLFM4* expression was associated with prostate cancer progression and with DNA methylation of CpG sites in the *OLFM4* gene promoter region in human prostate adenocarcinoma. We also found that OLFM4 may play a role in regulating EMT, as well as tumor initiation and growth, in prostate cells.

Materials and Methods

Human prostate tissue specimens and cell lines

Unstained whole-mount paraffin section slides of human prostate cancer tissues (for 31 primary prostate adenocarcinoma cases) were obtained from the Laboratory of Pathology, National Cancer Institute, National Institutes of Health (NIH, Bethesda MD). For each case, a pathologist (JR) reviewed the whole-mount sections and selected slides containing both cancer and normal regions.[33] We obtained adjacent normal cells (n = 8); lower grade tumor foci (LG, Gleason grade ≤3, n = 6); and higher-grade tumor foci (HG, Gleason grade ≥4, n = 8). Unstained paraffin section slides of human prostate cancer tissues (for 25 cases) were purchased from The Cooperative Human Tissue Network (CHTN, Mid-Atlantic Division, Charlottesville, VA). The clinical characteristics of the cases are summarized in Supporting Information Table S1. Human prostate cancer tissue array slides (for 70 prostate cancer cases and 10 normal tissues) were purchased from US Biomax (PR803, Rockville, MD). The clinical characteristics of the cases are summarized in Supporting Information Table S2.

The immortalized normal human prostate cell lines RWPE1 and RWPE2, which is established from RWPE1 by transforming with Kirsten murine sarcoma Ki-Ras, were purchased from the American Type Culture Collection (ATCC, Manassas, VA) and cultured in the recommended media.[34] Human prostate cancer cell lines PC-3 and DU145 were obtained from the ATCC and maintained in RPMI 1640 medium with 10% fetal bovine serum (ThermoFisher Scientific, Carlsbad, CA). Cell lines were characterized by the ATCC using morphology, karyotyping and polymerase chain reaction (PCR)-based approaches to authenticate the identity of cell lines. All cells were maintained at passage P2–P5 and were passaged for fewer than 6 months after receipt or resuscitation.

In some experiments, prostate cell lines were treated with 5 μM 5-aza-2′-deoxycytidine (5-Aza; Sigma-Aldrich, St. Louis, MO). Briefly, 1×10^6 cells were seeded in 10-cm plates and cultured with growth medium overnight. The 5-Aza-containing medium was replaced every 24 hr. Dimethyl sulfoxide (DMSO) was used as vehicle control.

Thirty-one human tissue slides were provided by laboratory of pathology, National Cancer Institute, National Institutes of Health and 25 human prostate cancer slides were purchased from The Cooperative Human Tissue Network (CHTN, Mid-Atlantic Division, Charlottesville, VA).

The data will be made available upon reasonable request.

Laser-capture microdissection

Laser-capture microdissection (LCM) was performed using an Arcturus Pix Cell II as previously described.[35] Using human prostate cancer tissues and matched adjacent normal tissues, microdissected cancerous and normal epithelial cells were identified from a total of 31 cases by a pathologist in the LCM core facility (National Cancer Institute). Approximately 10,000–15,000 laser shots were used for each case to procure the epithelial samples.[33]

Methylation analysis of the *OLFM4* gene promoter region

Genomic DNA purification from the LCM epithelial cell samples and prostate cell lines was performed as described

previously.[33] The methylation status of the eight CpG sites in the *OLFM4* gene promoter region was analyzed using Pyrosequence (EpigenDx, Hopkinton, MA).[17] Briefly, 1 μg of genomic DNA was bisulfite-treated with the EZ DNA methylation kit (Zymo Research, Irvine, CA). The DNA eluate was diluted 1:10, and 1 μl of the diluted DNA was then used for PCR with HotStar Taq Polymerase (Qiagen, Germantown, MD). Three pairs of PCR primers were designed to amplify the fragments that cover the eight CpG dinucleotide sites. The reverse PCR primer was biotin-labeled on the 5′-end and was purified by high-performance liquid chromatography. Pyrosequencing reactions were run on the PCR products using the PSQ 96HS system (Biotage, Charlottesville, VA). Pyro Q-CpG software (Biotage) was used to analyze the pyrosequencing data. The *OLFM4* gene promoter region primers used for PCR and pyrosequencing were as follows: ADS237 F: 5′-CCTCC TTGACTGGGTTTGAGGC-3′; ADS237FS: 5′-CCCTGGCC TGGGAG-3′; CpG sites: −681 and −666. ADS238 F: 5′-TGG TGAGATACTTGATAGGGCAGA-3′; ADS238FS1: 5′-GGTT GGCCAGGGAACAAA-3′; CpG site: −562. ADS238 F: 5′-T GGTGAGATACTTGATAGGGCAGA-3′; ADS238FS2: 5′-CA CTGTAAGGAACAGGTCAA-3′; CpG sites: −486 and −446. ADS239 F: 5′-GACTCAGATTCCTGGGTGTCCTG-3′; ADS239FS1: 5′-AACCTCCTGGGGCAGTTCACA-3′; CpG site: −91. ADS239 F: 5′-GACTCAGATTCCTGGGTGTCCTG-3′; ADS239FS2: 5′-CCTGGGCTCTCTGCAGAG-3′; CpG sites: +4 and +34.

Tumor xenografts

All animal experiments were approved by the Animal Care and Use Committee of the National Heart, Lung and Blood Institute (H-0266). Animal care was performed in accordance with relevant institutional and national guidelines and regulations in the animal facilities of the National Institutes of Health. *OLFM4*-expressing PC-3O cells or DU145O cells or vector-transfected control PC-3C cells or DU145C cells (2×10^6/0.1 ml RPMI mixed with 0.1 ml Matrigel [BD, Franklin Lakes, NJ]) were injected subcutaneously into the right flank of 6- to 8-week-old male NOD.CB17-Prkdc <SCID>/J mice (5 mice per each cell line; Jackson Laboratory, Ellsworth, ME).[15] Tumor growth was monitored after inoculation starting at 2 weeks and then every week thereafter. Volumes were calculated using the tumor volume = $(W^2 \times L)/2$ formula. All mice were euthanized at the same time point when the biggest tumor reached maximum size (2 cm^3) after inoculation, and all visible tumors were removed and weighed and/or photographed. Tumor tissues were frozen or fixed in 10% neutral buffered formalin solution (Sigma-Aldrich) and prepared for hematoxylin and eosin (HE) staining and immunohistochemistry.

Quantitative real-time RT-PCR

Quantitative real-time RT-PCR (qRT-PCR) was conducted as previously described.[15] Briefly, total RNA was extracted from prostate cells using RNeasy plus Mini kits (Qiagen). Total RNA (2 μg) was then reverse-transcribed using the SuperScript III First-Strand Synthesis System (ThermoFisher Scientific). TaqMan PCR primers and probes for *OLFM4* (Hs00197437_m1), *CDH1*(Hs01023894), *VIM* (Hs00958111) and the internal control *ACTB* (Hs01060665_g1) were purchased from Applied Biosystems (ThermoFisher Scientific). qRT-PCR was performed with QuantStudio 6 Flex (Applied Biosystems) using the following thermocycler protocol: 94°C for 10 min, followed by 40 cycles at 94°C for 10 sec, 60°C for 30 sec. Relative expression was calculated by a comparative CT method using the formula $2^{-\Delta\Delta CT}$.

Lentiviral particles short hairpin RNA interference

Lentiviral particles containing 3–5 expression constructs, each encoding a target-specific 19–25 nucleotide (plus hairpin) short hairpin RNA (shRNA) designed to knock down *OLFM4* gene expression (GC-1 shRNA (h) lentiviral particles; Cat# sc-75,113-V), were obtained from Santa Cruz Biotechnology, Inc (Dallas, TX). Control shRNA lentiviral particles-A (Cat# sc-108,080) were also obtained from Santa Cruz Biotechnology, Inc. The lentiviral particles were transduced into cells according to the manufacturer's instructions. The transduced cells were selected with puromycin (5 μg/ml, ThermoFisher Scientific) for 5 days.

Immunohistochemical staining

We previously generated and used an OLFM4 polyclonal antibody in immunohistochemistry and Western-blotting analyses of tumor cells and human tissues.[13,36] For these studies, whole-mount paraffin sections of human prostate tissues and xenograft tissue slides were deparaffinized, hydrated, and antigen retrieval performed with a high-pressure cooker (2100 Retriever, Electron Microscopy Science; Hatfield, PA) in 1× citrate buffer, pH 6.0.[18] Sections were incubated with primary OLFM4 antibody (1:500 dilution) overnight at room temperature, then incubated with biotinylated goat antirabbit secondary antibody (BioGenex, San Ramon, CA) for 1 hr followed by streptavidin–horseradish peroxidase complex (BioGenex) for 30 min at room temperature. Color was developed using 3,3′-diaminobenzidine (BioGenex), and sections were counterstained with Mayer's hematoxylin (Sigma-Aldrich). Expression patterns were blind-evaluated by two independent researchers. The intensity of expression was evaluated with MetaMorph software (MetaMorph Inc, Nashville, TN) that detected the brown color representing the expression of OLFM4 protein. Image J software (National Institutes of Health, Bethesda, MD) was used to count the nuclei counterstained by Mayer's hematoxylin. All images were acquired using an Olympus BX51 microscope (Olympus, Center Valley, PA) and Qimaging Camera with Q Capture pro software (Qimaging, Surrey, British Columbia, Canada).[15,18] Images were acquired using the 10× and 40× Uplan Apo objective,

then imported into Adobe Photoshop (San Jose, CA) for presentation.

Immunohistochemical staining of RWPE1 and RWPE2 cell xenograft tissues was performed using the following primary antibodies: anti-TWIST1 and anti-SNAIL1 (Novus Biologicals, Centennial, CO); anti-BMI1 (Abcam, Cambridge, MA); and anti-OLFM4, anti-E-cadherin and antivimentin (Cell Signaling Technology Inc, Danvers, MA). Secondary antibodies, Super Sensitive MultiLink and Super Sensitive Label were purchased from BioGenex. Dark brown color was developed with chromagen (BioGenex), and slides were counterstained with hematoxylin (Sigma-Aldrich). All images were acquired using an Olympus BX51 microscope (Olympus) and Qimaging Camera with Q Capture pro software (Qimaging). Images were acquired using the 10× or 40× Uplan Apo objective, then imported into Adobe Photoshop for presentation.

Western-blot analysis

Nuclear protein lysate extractions from prostate cancer cells were performed using NE-PER Nuclear and Cytoplasmic Extraction Reagents (ThermoFisher Scientific). Total proteins (25 μg) from nuclear or whole-cell extracts were separated electrophoretically using NuPAGE 4–12% Bis-Tris gels (Invitrogen), transferred to polyvinylidene difluoride membrane, and hybridized with anti-OLFM4 (Sino Biological Inc., Wayne, PA), anti-β-actin (Santa Cruz Biotechnology, Inc.), anti-TWIST1 (Novus Biologicals), or anti-ZEB1, anti-E-cadherin, anti-β-catenin, antivimentin or antihistone H3 (Cell Signaling Technology, Inc.) antibody overnight at 4°C. Membranes were then incubated with secondary antibody, and signal developed with Amersham ECL Western-blotting detection reagents (GE Healthcare, Chicago, IL).

Prostate sphere-formation assays

Prostate sphere-formation assays were performed following a previously described protocol.[37] Briefly, 1×10^4 prostate cancer cells were suspended in 50 μl PrEGM medium and mixed with 50 μl Matrigel, then cultured in 12-well plates for 12 days. The medium was changed every 48 hr. Images of spheres were captured with an IX81 microscope (Olympus) using a 40× objective and Slide Book software system (Olympus) at 12 days, and green fluorescent protein (GFP)-positive colonies larger than 50 μm in diameter were counted.

Generation of stably expressing *OLFM4*-GFP tag-expressing prostate cancer cell clones

We have previously verified that human prostate cancer cells lack *OLFM4* expression.[15] The pCMV-6-AC-GFP tag-vector and pCMV-6-*OLFM4*-GFP tag plasmids were purchased from Origene (Rockville, MD). Stably expressing *OLFM4*-GFP tag-expressing prostate cancer cell clones (O) or vector-GFP tag-transfected control prostate cancer cell clones (V) were established following previously described protocols.[15,33]

Colony formation in soft agar

Stably expressing *OLFM4*-GFP tag-expressing PC-3 cell clone (PC-3O) or vector-GFP tag-transfected control PC-3 cell clone (PC-3 V) cell suspensions (1×10^4 cells/mL) in 2 ml of 0.35% Noble agar with RPMI containing 10% fetal bovine serum were overlaid into six-well plates containing a 0.6% agar base. The medium on top of the agar was changed every 48 hr. Images of colonies were captured with an IX81 microscope with a 5× objective and Slide Book software system on Day 14, and GFP-positive colonies larger than 50 μm in diameter were counted.[38,39]

OLFM4 promoter reporter-activity assays

pGL3-*OLFM4* reporter plasmids were constructed as previously described.[40,41] pGL3 basic vector control and pGL3-*OLFM4* reporter plasmids were then methylated by treatment with CpG methyltransferase (M. SssI, EM0821, ThermoFisher Scientific) following the industry's instructions and verified using restriction enzyme-digestion methods with Hpa II (undigested) and Msp I (digested). The methylated DNA plasmids were then purified using plasmid DNA spin columns (QIAprep Spin miniprep Kit, Qiagen).

For transient transfection of these reporter plasmids, PC-3 cells (1×10^5/well) were first seeded into 24-well plates (FALCON) and cultured for 1 day in growth medium. Transient transfection was then performed using Lipofectamine 2000 (ThermoFisher Scientific, #11668-019) following the manufacturer's instructions. After 48 hr of transfection, cells were lysed with 1x passive buffer and promoter activity measured with a dual-luciferase assay reporter assay system (Promega, Madison, WI, #E1910), using a TD 20/20 luminometer (Promega). The relative promoter activity was shown by using firefly luciferase activity normalized with *Renilla* Luciferase activity.

Bioinformatics analysis

Demographic, clinical and pathological data for 333 primary prostate adenocarcinoma patients were downloaded from The Cancer Genome Atlas (TCGA; www.cbioportal.org) and summarized as means and ranges as appropriate. Normalized mRNA expression data for the *OLFM4* gene were downloaded from TCGA for 333 primary prostate adenocarcinoma patients[4] and from the GSE21032 dataset for 174 prostate adenocarcinoma patients.[42] Recurrence-free survival data were downloaded from the GSE21032 dataset.[42]

Statistical analysis

Statistical analyses were performed using GraphPad Prism 5.0 software (La Jolla, CA) or SAS software version 9.1 (Cary, NC). Comparisons of OLFM4 expression were performed with one-way analysis of variance (ANOVA). Comparisons of *OLFM4* gene promoter region methylation levels, prostate sphere or colony formation, xenograft tumor weight and vimentin mRNA expression were performed with Student's

t-test. The relationships between *OLFM4* expression and methylation of the *OLFM4* gene promoter region were analyzed using Pearson's analysis with open-source R packages. The univariate and multivariate proportional hazards analysis used in Supporting Information Table S3. Recurrence-free survival data were analyzed with Kaplan–Meier plots and the log-rank test. A *p*-value of ≤0.05 was considered statistically significant.

Results

Reduced OLFM4 expression is associated with higher Gleason scores, increased preoperative serum PSA levels and significantly lower recurrence-free survival in human primary prostate adenocarcinoma

We initially examined OLFM4 protein expression in whole-mount sections of human prostate cancer tissues containing matched normal tissues adjacent to primary tumors in those specimens by immunohistochemical staining with OLFM4 antibody (Fig. 1*a*). compared to normal prostate tissue adjacent to primary tumors, OLFM4 protein expression was reduced in both lower grade tumor (LT: Gleason grade, GL. 3) and higher-grade tumor (HG: Gleason grade, GL. 4) prostate cancer tissues foci (Fig. 1*a*). Quantitation of OLFM4 protein expression in a larger number of human prostate cancer tissues from two well-characterized populations indicated that OLFM4 was significantly reduced in prostate cancer tissues when compared to adjacent normal tissues (Fig. 1*b*). To extend upon these observations, we downloaded OLFM4 mRNA expression data and clinical data for 181 prostate adenocarcinoma patients (GSE21032 dataset) and 333 primary prostate adenocarcinoma patients (TCGA Cell 2015). In

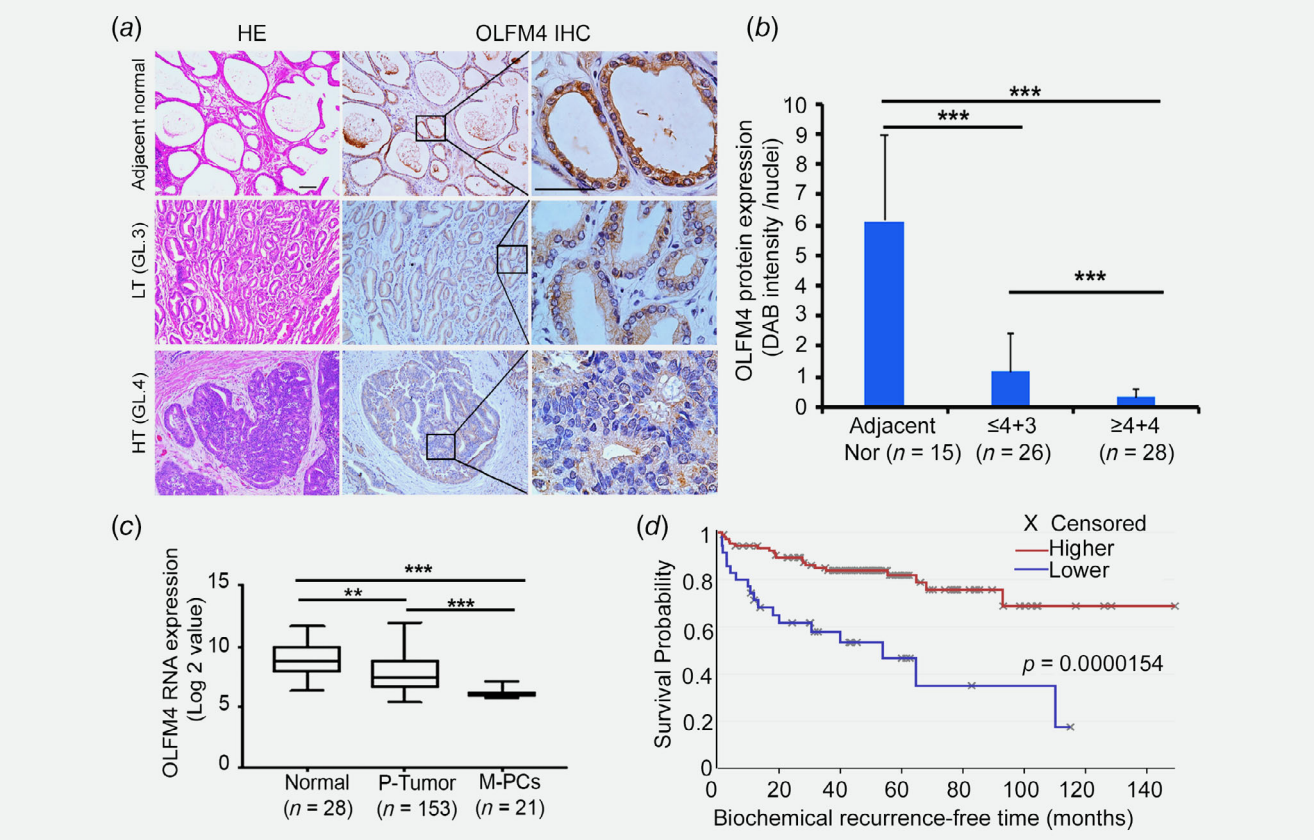

Figure 1. Reduced OLFM4 expression is associated with higher Gleason scores and lower recurrence-free survival in human primary prostate adenocarcinoma. (*a*) Representative images of HE staining and immunohistochemistry (IHC) analysis of OLFM4 protein expression in adjacent normal and tumor regions of whole-mount section human prostate cancer tissue specimens (obtained from the Laboratory of Pathology, National Cancer Institute). All micrographs shown are for tissues obtained from the same case. LT, lower grade tumor (Gleason grade 3, GL. 3); HT, higher grade tumor Gleason grade 4, GL. 4). Scale bars: 50 μm. (*b*) Quantitation of OLFM4 protein expression from immunohistochemical analyses using human prostate cancer tissue slides obtained from CHTN and US Biomax. Data represent the mean ± standard deviation (SD) of 3,3′-diaminobenzidine (DAB) intensity normalized to the number of nuclei. Adjacent Nor., normal tissue adjacent to primary tumor; Gleason score ≤4 + 3; Gleason score ≥4 + 4. We excluded CHTN and US Biomax cases with quality issues for which we could not obtain immunohistochemistry data. ***$p \leq 0.001$ (ANOVA). (*c*) OLFM4 mRNA expression in prostate cancer specimens in data downloaded from the GSE21032 dataset. Data represent the mean ± SD. Normal, normal tissue adjacent to primary tumor; P-tumor, primary tumor; M-PCs; prostate tumor with distant metastasis. **$p \leq 0.01$; ***$p \leq 0.001$ (ANOVA). (*d*) Kaplan–Meier plot of recurrence-free survival for OLFM4 mRNA higher-expressing (red line) and lower-expressing (blue line) prostate adenocarcinoma patient cohorts in the GSE21032 dataset at 25% thresholds ($p = 0.0000154$; log-rank test).

GSE21032 data, OLFM4 mRNA expression was significantly reduced in primary prostate cancer tumors and metastatic prostate cancer tumors compared to normal prostate tissue; furthermore, OLFM4 mRNA expression in metastatic tumors was significantly lower than that observed in primary prostate cancer tumors (Fig. 1*c*).

To evaluate the clinical impacts of the *OLFM4* gene in prostate cancer, we performed bioinformatic analyses with the primary prostate adenocarcinoma data downloaded from TCGA Cell 2015. Analyses of the relationship between *OLFM4* expression and clinicopathological parameters for these patients indicated that *OLFM4* expression was not

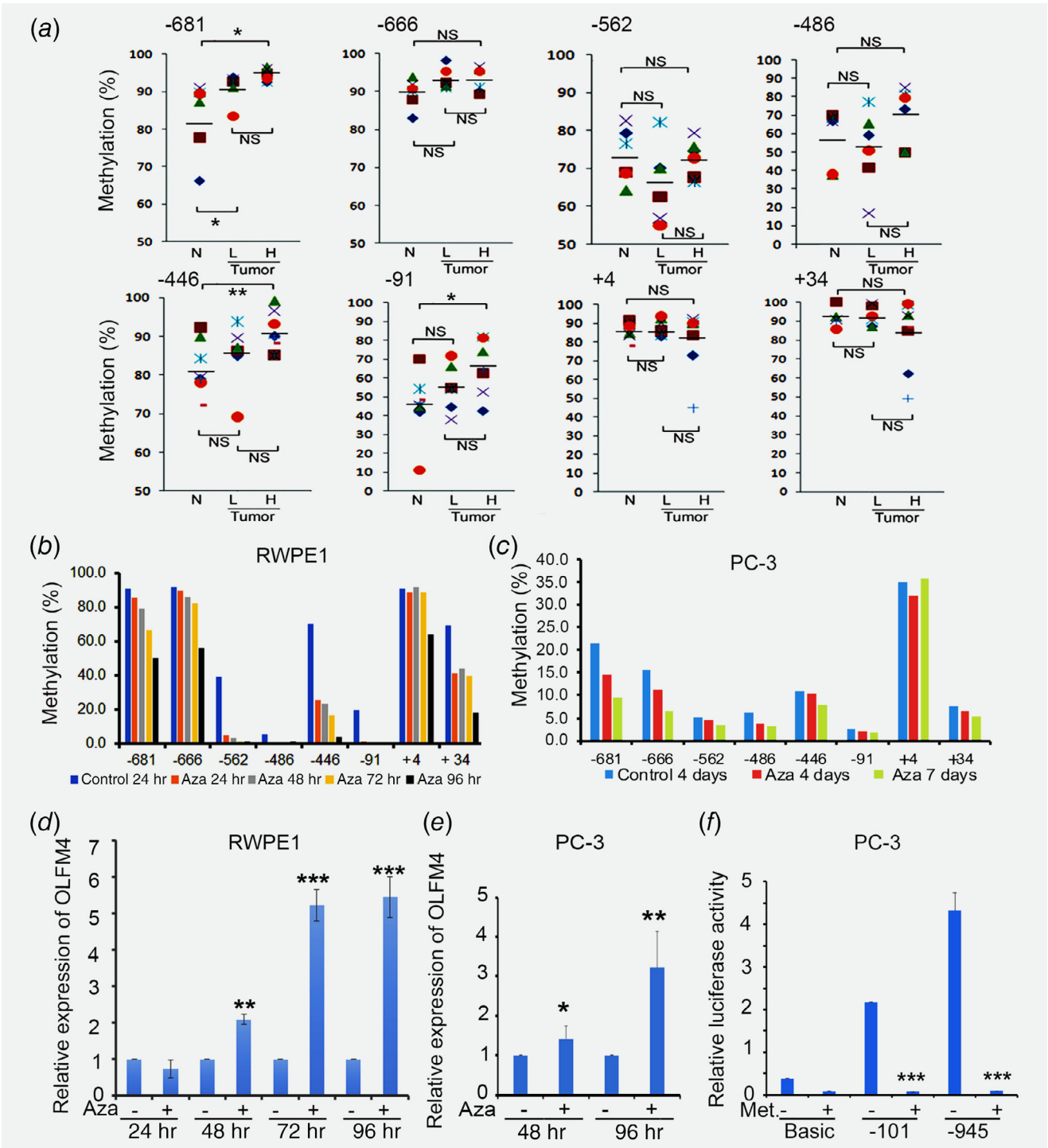

Figure 2. Legend on next page.

significantly different between two age cohorts (60 years old and under and above 60 years old), and between two ERG translocation cohorts (ERG fusion-positive and ERG fusion-negative). Interestingly, *OLFM4* expression was significantly lower in patients with a preoperative serum PSA level above 20 ng/ml (compared to those with a PSA at or below 20 ng/ml) and in patients with a tumor with a Gleason score of ≥4 + 4 (compared to those with a tumor with a Gleason score of ≤3 + 4; Table 1). *OLFM4* expression level was similar in patients with a surgical margin resection R1–2 compared to patients with a surgical margin resection R0 (Table 1).

We next analyzed the relationship between OLFM4 mRNA expression and recurrence-free survival in the GSE21032 patient cohort (Visualization: Samples 131/181; Censored 103/131) and found that patients in the lower OLFM4 mRNA expression cohort (lower 25%) had significantly lower recurrence-free survival than those patients in the higher OLFM4 mRNA expression cohort (higher 75%; Fig. 1*d*). Furthermore, we performed univariate and multivariate Cox regression hazard analysis with GSE 21032 data set for predictive effect of OLFM4 expression on post-operative biochemical recurrence-free survival (Supporting Information Table S3). Lower OLFM4 expression was significantly associated with worse recurrence-free survival (HR = 3.18; 95% CI 1.55–6.51; p = 0.0016, Supporting Information Table S3). Besides expression level of OLFM4, Gleason scores and preoperative PSA level was stronger associated with biochemical recurrence-free survival (Supporting Information Table S3). In the multivariate Cox regression hazard analysis, OLFM4 expression level after adjusting for Gleason score was not significant (HR = 1.70; 95% CI 0.80–3.59; p = 0.17; Supporting Information Table S3). The patient cohort examined was reduced from the full 181–131 patient cohort based on availability of all clinical parameters and Gleason score categories used.

Reduced OLFM4 mRNA expression is associated with CpG site increased methylation of the *OLFM4* gene promoter region in primary prostate adenocarcinoma

To investigate the DNA methylation status of the promoter region of the *OLFM4* gene in human prostate cancer, we obtained epithelial cells from whole-mount sections of human prostate cancer specimens using LCM. The promoter region of the *OLFM4* gene has eight CpG sites (−681, −666, −562, −486, −446, −91, +4 and +34, relative to the *OLFM4* transcription start site). The heterogeneities of the methylation status of the eight CpG sites in the *OLFM4* gene promoter region were determined from analyses of paired tumor cells and adjacent normal cells obtained from primary prostate adenocarcinoma cases. We excluded cases that either had no paired cells or those for which we could not obtain methylation data. Among the eight CpG sites, three sites (−681, −446 and −91) were hypermethylated in the higher grade tumor cells compared to adjacent normal cells in the patients studied (Fig. 2*a*), while no significant difference in methylation was observed when higher grade tumor cells were compared to adjacent normal cells for the other five CpG sites (−666, −562, −486, +4 and +34; Fig. 2*a*). Summarized results for immunohistochemistry and methylation status analyses in individual patients indicated that specimens with lost OLFM4 protein expression also exhibit increased methylation of the −681, −446 and −91 CpG sites in the *OLFM4* gene promoter region (Supporting Information Table S4).

Treatment with the methylation inhibitor 5-aza-2′-deoxycytidine increased OLFM4 mRNA expression in human prostate cell lines

To test whether blocking methylation of CpG sites in the *OLFM4* gene promoter region can induce *OLFM4* gene expression, we tested the effect of CpG site methylation on OLFM4 expression by treating RWPE1 and PC-3 prostate cells with the methylation inhibitor 5-Aza (5 μM) for 24–96 hr. compared to control-treated cells, 5-Aza treatment of RWPE1 cells and PC-3 cells decreased methylation of 8 CpG sites (except +4 site only observed at 96 hr in RWPE1 cells) in the *OLFM4* gene promoter region (Figs. 2*b* and 2*c*). OLFM4 mRNA expression was significantly increased after treatment with 5-Aza for 48, 72 or 96 hr in RWPE1 and for 48 and 96 hr in PC-3 cell lines compared to DMSO (vehicle control)-treated cells (Figs. 2*d* and 2*e*). These results suggest

Figure 2. Reduced OLFM4 expression is associated with CpG site increased methylation of the OLFM4 gene promoter region in human prostate adenocarcinoma and prostate cell lines. (*a*) OLFM4 promoter region CpG site methylation status in DNA isolated from epithelial cells obtained from prostate cancer specimens using LCM. Methylation levels in adjacent normal prostate epithelial cells (N), lower grade prostate cancer cells (L) and higher-grade prostate cancer cells (H) were measured using pyrosequencing. Data represent the mean ± SD (N = 5–8; L = 5–6; H = 6–8). The difference between pairs of groups was analyzed using Student's *t*-test. *$p \le 0.05$; **$p \le 0.01$; NS, not significant. (*b* and *c*) Methylation status (percentage) of the eight CpG sites (−681, −666, −562, −486, −446, −91, +4 and +34, relative to the OLFM4 transcription start site) in the OLFM4 gene promoter region. RWPE1 cells were treated with Aza (5 μM) for 24, 48, 72 or 96 hr (*b*) and PC-3 cells were treated with Aza (5 μM) for 4 and 7 days. (*d*) Relative expression of OLFM4 mRNA in RWPE1 cells determined by qRT-PCR after treatment with Aza (5 μM) or control (DMSO) for 24, 48, 72 or 96 hr. (*e*) Relative expression of OLFM4 mRNA in PC-3 cells determined by qRT-PCR after treatment with Aza (5 μM) or control (DMSO) for 48 or 96 hr. (*d*, *e*) Data represent the mean ± SD of three experiments performed in triplicate. The difference between Aza treatment and vehicle at each time point was analyzed using the Student's *t*-test. *$p \le 0.05$; **$p \le 0.01$; ***$p \le 0.001$. (*f*) OLFM4 promoter reporter activity. pGL3 basic vector control, −101 pGL3-OLFM4 reporter plasmid, and −945 pGL3-OLFM4 reporter plasmid were treated without (Met −) or with CpG methyltransferase (Met +). Data represent the mean (±SD, n = 3) relative luciferase activities of these plasmids after their transient transfection into PC-3 cells. The difference between treated without (Met −) or with CpG methyltransferase (Met +) was analyzed using the Student's *t*-test. ***$p \le 0.001$.

Table 1. Relationship between OLFM4 mRNA expression and clinicopathological parameters in 333 primary prostate adenocarcinoma patients

Variable	All patients	Mean OLFM4 expression (Log2)	*p*-value[1]
Age (61 ± 7 years)[2]			
All	279[3]	8.80 ± 3.37	
‹60	120	8.68 ± 3.41	
≥60	159	8.89 ± 3.34	0.61
Preoperative PSA (11.0 ± 11.2 ng/ml)			
All	187[3]	9.23 ± 3.25	
≤20	164	9.55 ± 3.16	
›20	23	7.01 ± 3.10	0.0004[4]
Gleason score			
All	333	8.78 ± 3.29	0.0092
≤3 + 4	167	9.11 ± 3.22	
4 + 3	78	9.12 ± 2.74	
≥4 + 4	88	7.87 ± 3.72	0.014[5]
Surgical margin resection			
All	262[3]	8.81 ± 3.39	
R0	193	8.90 ± 3.43	
R1–2	69	8.55 ± 3.27	0.47
ERG translocation			
All	333	8.78 ± 3.29	
ERG fusion-positive	152	9.11 ± 3.14	
ERG fusion-negative	181	8.51 ± 3.40	0.10

Data for 333 primary prostate adenocarcinoma patients were downloaded from TCGA.[4]
[1]*p* values are from *t*-test or analysis of variance (Gleason score).
[2]Mean ± standard deviation.
[3]Number of patients with data available in the 333-patient cohort.
[4]In multivariable regression, for PSA adjusting for Gleason score, $p = 0.0022$.
[5]Gleason score ≥4 + 4 *vs*. 4 + 3.

that CpG site methylation status of the *OLFM4* gene promoter region correlates with OLFM4 expression levels in human prostate cells.

Methylation of CpG sites in the *OLFM4* promoter region reduced *OLFM4* promoter activity

To test whether methylation of the CpG sites in the *OLFM4* promoter affects its activity, we performed *OLFM4* promoter reporter-activity assays. We utilized several pGL3-*OLFM4* reporter plasmids that included different segments of the *OLFM4* promoter region in order to examine the effects of methylation of CpG sites in the promoter (Supporting Information Fig. S1*a*).[40] Luciferase assays conducted after transient transfection of PC-3 cells with the different *OLFM4* promoter-reporter plasmids indicated that all the constructs except the −66 reporter plasmid exhibited increased promoter activity compared to basic vector control-transfected cells (Supporting Information Fig. S1*b*). Subsequent analyses utilized pGL3-basic vector, −101 (which included CpG site −91) and −945 which included CpG sites −681, −446 and −91 pGL3-*OLFM4* reporter plasmids treated with or without CpG methyltransferase. Methylation of the CpG sites in these reporter plasmids significantly reduced *OLFM4* promoter reporter activities, compared to vehicle-treated plasmids, after transient transfection of these plasmids into PC-3 cells (Fig. 2*f*). These results directly verified that methylation of the CpG sites in the *OLFM4* promoter region significantly reduced *OLFM4* promoter activity.

Knockdown of *OLFM4* expression is associated with enhanced EMT-marker expression in RWPE cells

To study the biological functions of *OLFM4* in human normal prostate epithelial cells, we used shRNA interference to knock down the *OLFM4* gene in two RWPE cell lines. In untreated cells, OLFM4 mRNA expression level was higher in RWPE1 cells when compared to RWPE2 cells (Fig. 3*a*). Knockdown effectively decreased expression of OLFM4 in RWPE1 cells and RWPE2 cells at the mRNA (Fig. 3*b*).

We have previously reported that *Olfm4* knockout mice displayed high expression of EMT markers in prostate tissue.[33] Therefore, we examined EMT-marker expression in *OLFM4*-knockdown RWPE cells. Expression of vimentin, but not E-cadherin, mRNA was significantly increased in *OLFM4*-knockdown RWPE1 and RWPE2 cells compared to control shRNA-knockdown cells (Fig. 3***c***). At the protein level, E-cadherin protein levels were reduced, while vimentin and

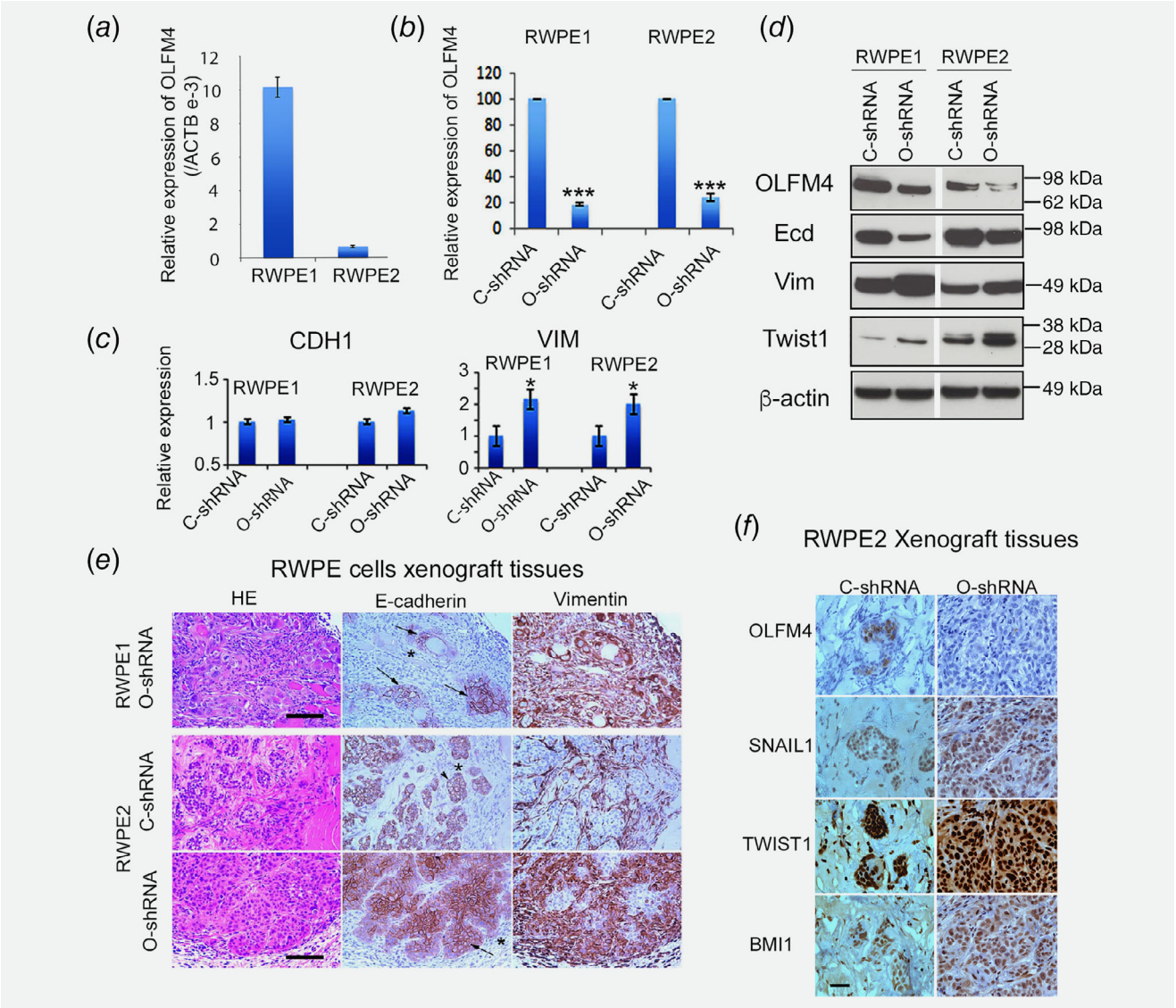

Figure 3. Knockdown of OLFM4 expression is associated with enhanced EMT-marker expression in RWPE cells. (*a*) Expression of OLFM4 mRNA in RWPE1 and RWPE2 cells determined by qRT-PCR. Values relative to β-actin (ACTB) represent the mean ± SD of three experiments performed in triplicate. (*b*) RWPE1 or RWPE2 cells were knocked down with control shRNA (C-shRNA) or OLFM4 shRNA (O-shRNA). Expression of OLFM4 mRNA determined by qRT-PCR in knockdown RWPE1 and RWPE2 cells. Values normalized to ACTB represent the mean ± SD of three experiments performed in triplicate compared to control shRNA-knocked-down cells (value set at 100%). (*c*) Relative expression of E-cadherin (CDH1) and vimentin (VIM) mRNA determined by qRT-PCR in OLFM4- or control-knockdown RWPE1 and RWPE2 cells. Data represent the mean ± SD of three experiments performed in triplicate compared to control shRNA-knocked-down cells (value set at 1). *$p \leq 0.05$ (Student's *t*-test). (*d*) Western-blot analysis of OLFM4, E-cadherin (Ecd), vimentin (Vim) and TWIST1 in OLFM4 (O) or control (C) knockdown RWPE1 and RWPE2 cells. β-actin was used as a loading control. (*e*) Representative images of HE staining and immunohistochemistry analysis of E-cadherin and vimentin expression in xenograft tissues that emerged in mice after subcutaneous inoculation with OLFM4- or control shRNA-knockdown RWPE cells. Arrow indicates EMT cells; arrow head indicates Epithelial cells; Star indicates stromal cells. Scale bar: 100 μm. (*f*) Representative images of immunohistochemistry analysis of OLFM4, TWIST1, SNAIL1 and BMI1 expression in xenograft tissues that emerged in mice after subcutaneous inoculation with OLFM4-knockdown RWPE2 cells. Scale bar: 50 μm.

TWIST1 protein levels were increased, in *OLFM4*-knockdown RWPE1 and RWPE2 cells (Fig. 3*d*). Using an *in vivo* xenograft tumor model in which *OLFM4*-knockdown or control shRNA-knockdown RWPE cells were inoculated subcutaneously into mice and the tumors that emerged then examined, we observed increased vimentin staining in xenograft tissues obtained from *OLFM4*-knockdown RWPE1 and RWPE2 cells compared to control shRNA-knockdown RWPE2 cells (Fig. 3*e*). *OLFM4*-knockdown RWPE2 cells in xenograft tissues also strongly expressed the EMT transcription factors TWIST1, SNAIL1 and BMI1 (Fig. 3*f*). These results suggest that knockdown of *OLFM4* is associated with increased

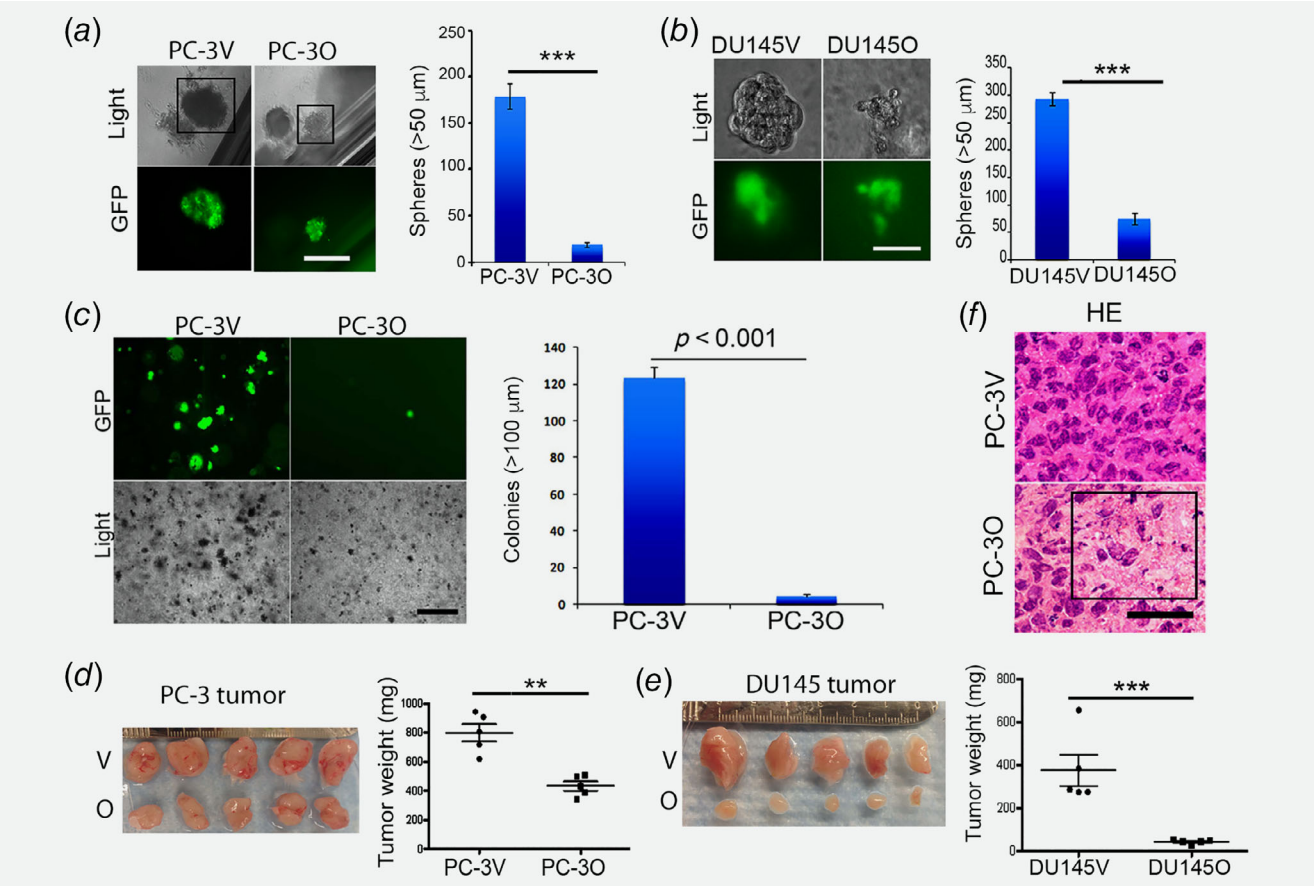

Figure 4. Restoration of OLFM4 expression in prostate cancer cells inhibited tumor cell growth in vitro and xenograft tumor growth in mice. The stably expressing prostate cancer cell clones PC-3V (vector-GFP tag), PC-3O (OLFM4-GFP tag), DU145V (vector-GFP tag) and DU145O (OLFM4-GFP tag) were established. (*a*, *b*) Stably expressing prostate cancer cell clones were subjected to prostate sphere-formation assays. Spheres were photographed after culturing for 12 days with Matrigel in 12-well plates. Photographs were taken of identical fields under light (Light) and fluorescent (GFP) conditions. Squares in the top row of PC-3 cell micrographs indicate GFP-positive spheres. Scale bars: 200 μm. Bar graphs represent the mean number (±SD) of spheres (›50 μm in diameter) per well counted from six wells for each cell clone. (*c*) Stably expressing PC-3 prostate cancer cell clones were grown in soft agar to support colony formation. PC-3V and PC-3O cell colonies were photographed after 14 days in culture. Photographs were taken of identical fields under light (Light) and fluorescent (GFP) conditions. Scale bar: 200 μm. Bar graph represents the mean number (±SD) of colonies formed ($n = 6$). (*d*, *e*) Stably expressing prostate cancer cell clones were used to inoculate mice in tumor xenograft studies. The xenograft tumors that emerged after inoculation were dissected, photographed, and weighed; PC-3 tumors were dissected 19 days after inoculation, and DU145 tumors were dissected 42 days after inoculation. Scott plot graphs represent the weights of the xenograft tumors shown in the photographs ($n = 5$). The difference between pairs of groups in all panels was analyzed using Student's *t*-test. (*f*) Representative HE-stained images from PC-3 xenograft tumors. Box indicates area with fewer cells. Scale bar: 50 μm.

expression of EMT markers and transcription factors in RWPE cells.

Restoration of *OLFM4* expression inhibited *in vitro* prostate cancer cell growth and *in vivo* xenograft tumor growth in mice

To investigate whether restoration of *OLFM4* expression can affect tumor-formation ability in these cells, we grew PC-3 and DU145 cells carrying either a vector-GFP tag plasmid or an *OLFM4*-GFP tag plasmid in three-dimensional (3D) Matrigel cultures. We traced cell growth by the expression of the GFP tag and found that restoration of *OLFM4* expression in these cells significantly inhibited prostate sphere formation *in vitro* (Figs. 4*a* and 4*b*). In parallel *in vitro* experiments examining colony formation in soft agar, PC-3 cells expressing *OLFM4* formed significantly fewer colonies compared to PC-3 cells expressing the vector-GFP tag (Fig. 4*c*).

We further explored the effects of *OLFM4* expression on prostate cancer cell growth *in vivo* in our tumor xenograft model. When PC-3 or DU145 cells carrying either a vector-GFP tag plasmid or an *OLFM4*-GFP tag plasmid were inoculated subcutaneously into mice, the tumors that emerged from *OLFM4*-expressing cells were significantly smaller than those that emerged from cells expressing the vector-GFP tag,

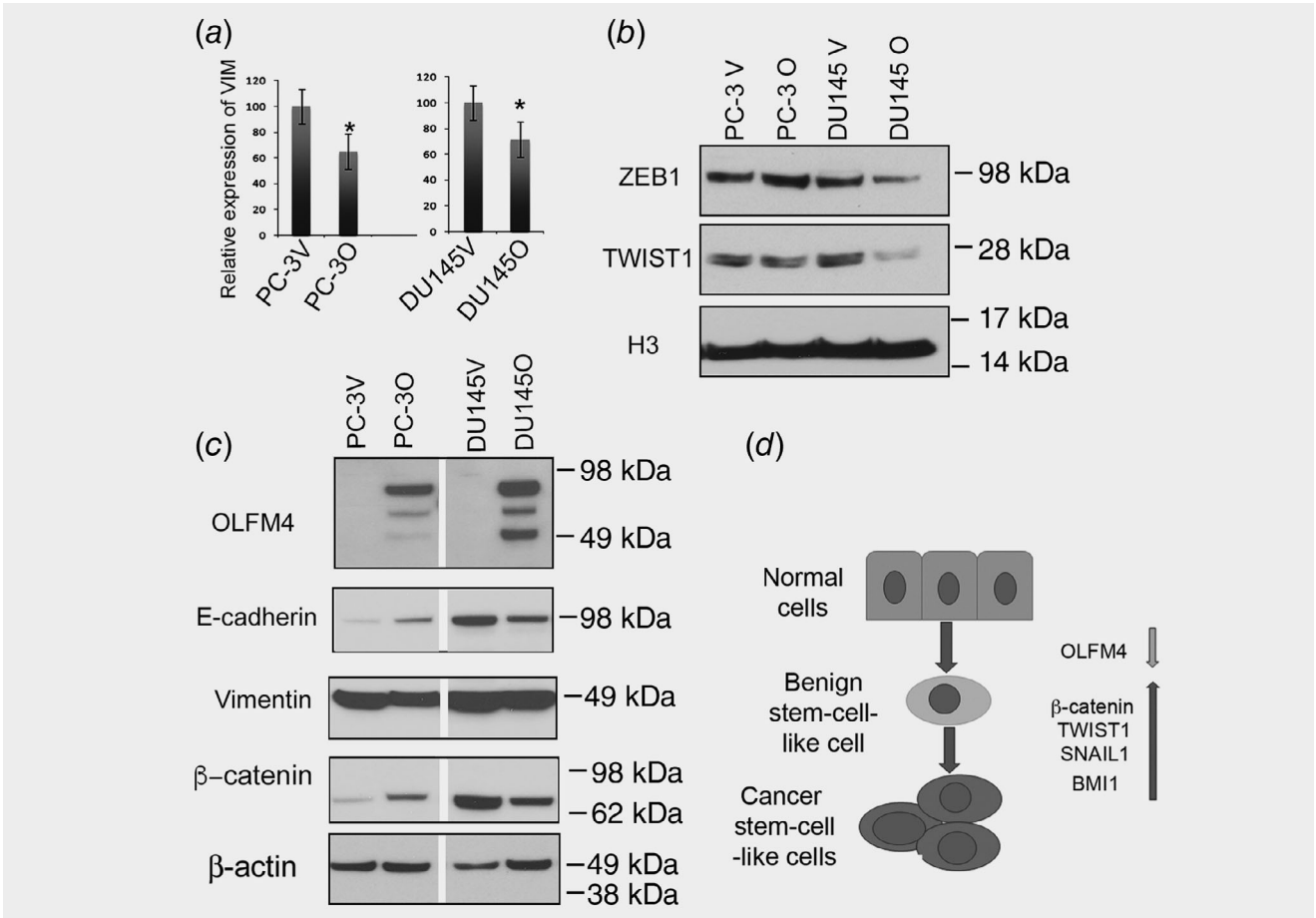

Figure 5. Restoration of OLFM4 expression in prostate cancer cells inhibited EMT-marker expression. (*a*) Relative expression of vimentin (VIM) mRNA determined by qRT-PCR in stably expressing *OLFM4*-GFP tag-expressing (O) or vector-GFP tag-transfected control (V) PC-3 and DU145 prostate cancer cell clones. Data represent mean ± SD percent expression in OLFM4-GFP tag-expressing cell clones compared to vector-GFP tag-expressing cell clones (value set at 100%; $n = 3$). The difference between pairs of groups was analyzed using Student's *t*-test. $*p \leq 0.05$. (*b*) Western-blot analysis of OLFM4, E-cadherin, vimentin and β-catenin in total cell lysates from prostate cancer cell clones. β-actin was used as a loading control. (*c*) Western-blot analysis of ZEB1 and TWIST1 in nuclear extracts from prostate cancer cell clones. Histone H3 was used as a loading control. (*d*) Proposed model of relationship between OLFM4 and EMT-regulating proteins in benign and cancer stem-cell-like cells in the prostate.

indicating that *OLFM4* expression inhibited xenograft tumor growth *in vivo* (Figs. 4*d* and 4*e*). Cell growth was diminished in tumor tissues emerging from *OLFM4*-expressing PC-3 cells compared to those emerging from vector-expressing (control) PC-3 cells (Fig. 4*f*). Collectively, these results suggest that OLFM4 inhibits tumor-formation ability in prostate cancer cells.

Restoration of *OLFM4* expression inhibited EMT-marker expression in prostate cancer cells

We have previously demonstrated that OLFM4 suppresses human prostate cancer cell growth and metastasis *via* negative interactions with stromal cell-derived factor-1 (SDF-1), cathepsin D[15,33] and sonic hedgehog (SHH) proteins.[43] Here, when we restored *OLFM4* expression in the prostate cancer cells PC-3 and DU145, vimentin expression was reduced at both the mRNA and protein levels (Figs. 5*a* and 5*b*). Expression of E-cadherin protein after restoration of *OLFM4* expression was increased in PC-3 cells but decreased in DU145 cells, but expression of β-catenin protein was reduced in both *OLFM4*-expressing PC-3 and DU145 cells compared to those expressing a vector-GFP tag (Fig. 5*b*). When we examined expression of EMT transcription factors in these cells, we found that *OLFM4* expression reduced TWIST1 protein expression in nuclear extracts from PC-3 and DU145 cells, but reduced ZEB1 expression only in DU145 nuclear extracts (Fig. 5*c*). Collectively, these results suggest that OLFM4 inhibits the EMT in prostate cancer cells.

Discussion

We provide evidence here that downregulation of OLFM4 expression is associated with tumor initiation, growth and

progression of prostate cancer. Our bioinformatic studies with clinical datasets establish that reduced OLFM4 mRNA expression is associated with higher preoperative serum PSA levels, higher Gleason scores and lower recurrence-free survival in human prostate cancer patients. Thus, OLFM4 may be useful as a novel candidate biomarker for prostate cancer.

OLFM4 mRNA and protein expression in normal and cancerous prostate tissues and cell lines have been evaluated in our laboratory previously.[15,33] We observed that loss or reduction of OLFM4 expression was associated with higher Gleason scores of prostate cancer and prostate cancer cell lines such as PC-3 and DU145.[15,18] The *OLFM4* gene was deleted in approximately 25% of human prostate cancer specimens that we studied.[33] When we further investigated the alteration of the *OLFM4* gene through bioinformatics studies for clinical datasets of human prostate cancers, we found that the *OLFM4* gene was deleted in 10–25% of prostate cancer tissues in The Cancer Genome Atlas (TCGA) patient cohort, and that expression of *OLFM4* was lost in more than 50% of prostate samples obtained from advanced prostate cancer patients.[14,15,18] Therefore, we sought to identify factors other than DNA deletion that may be involved in the reduced *OLFM4* expression observed in human prostate cancer progression.

DNA methylation is abnormally regulated in many cancer types, including prostate cancer.[44] We found here that increased CpG site methylation in the *OLFM4* gene promoter region was associated with reduced expression of *OLFM4*, which is similar to what has been observed for tumor-suppressor genes (e.g., *APC*, *RASSF1A* and *GSTP1*) during the progression of prostate cancer.[45,46] Importantly, we have identified three CpG sites (−681, −446 and −91) that were increased methylation in the high-grade prostate cancer tissues examined. Therefore, we provided evidence that downregulation of OLFM4 expression was also associated with the status of CpG site methylation of OLFM4 promoter in prostate cancer progression. In summary, downregulation of OLFM4 expression might be involved in both deletion and methylation of OLFM4 gene in the prostate cancer progression.

It has previously been shown that immortalized normal prostate epithelial cells retain properties of stem/progenitor cells and can be transformed to mimic progression of prostate cancer.[47,48] In addition, prostate cancer cells PC-3 and DU145 have been shown to express EMT markers and the EMT transcription factor TWIST1,[10] but to lose *OLFM4* expression.[15] In our study, we found that knockdown of *OLFM4* expression in RWPE cells enhanced EMT-marker expression in both *in vitro* cultures and xenograft tissues *in vivo*. We further demonstrated that restoration of *OLFM4* expression in PC-3 and DU145 cells inhibited their expression of vimentin and TWIST1, as well as significantly inhibited their ability to form prostate spheres in 3D Matrigel cultures *in vitro* and tumors in an *in vivo* xenograft tumor model. These findings suggest that OLFM4 may be involved in regulating the EMT program and tumor initiation in prostate cancer cells.

We have previously reported that OLFM4 plays tumor-suppressor roles in both prostate cancer cell lines and the murine prostate in an *Olfm4* knockout mouse model.[15,33,43] We and other groups have also reported OLFM4 tumor-suppressor functions in colon cancer, mouse melanoma cells and early gastric cancer.[16,49–51] Studies of the molecular mechanisms underlying OLFM4 tumor-suppressor function have revealed that OLFM4 negatively regulates cathepsin D, SDF-1 and SHH signaling pathways during the progression of prostate cancer.[15,43] OLFM4 suppresses prostate cancer growth and metastasis by directly interacting with cathepsin D (thereby downregulating cathepsin D enzyme activity) and inhibits prostate cancer cell invasion and metastasis by interacting with SDF-1 (thereby downregulating SDF-1/CXCR4 signaling).[15] OLFM4 protein also inhibits prostate carcinogenesis and is associated with downregulation of the SHH-signaling pathway *via* binding to SHH protein.[43] The SHH pathway's key transcription factors GLI1 and GLI2 have been shown to activate EMT transcription factors, such as SNAIL1, ZEB1 and FOXC2, as well as the stem-cell self-renewal polycomb family member BMI1.[52] We have demonstrated here that downregulation of OLFM4 enhanced expression of EMT proteins and the stem-cell marker BMI1 in normal prostate epithelial cells, which may induce them to become EMT stem-cell-like cells and further progress towards malignant stem-cell-like cells (Fig. 5*d*).

Taken together, these data suggest that OLFM4 plays a critical tumor-suppressor role underlying the progression of primary prostate cancer. The clinical correlation between reduced OLFM4 expression level and higher preoperative serum PSA levels, higher Gleason scores and lower recurrence-free survival in prostate cancer patients suggest that OLFM4 might be useful as a novel candidate biomarker for prostate cancer. Further clinical studies of the *OLFM4* gene as a candidate biomarker for prostate cancer will need to be evaluated with large cohort studies of prostate cancer patients.

Acknowledgements

We thank Drs Christian A. Combs and Daniela Malide (Light Microscopy Core Facility, National Heart, Lung and Blood Institute, National Institutes of Health) for help with immunohistochemistry image quantitation and Dr Elizabeth Wright (National Institute of Diabetes and Digestive and Kidney Diseases, National Institutes of Health) for help with statistical analysis. We thank Drs Weiping Chen (Genomics Core Facility, National Institute of Diabetes and Digestive and Kidney Diseases, National Institutes of Health) and Mehdi Pirooznia (Bioinformatics and Systems Biology Core, National Heart, Lung and Blood Institute, National Institutes of Health) for their help with GSE21032 and TCGA data download and analysis. This work was supported by the Intramural Research Program, National Institutes of Health/National Institute of Diabetes and Digestive and Kidney Diseases.

References

1. Siegel RL, Miller KD, Jemal A. Cancer statistics, 2016. *CA Cancer J Clin* 2016;66:7–30.
2. Ngollo M, Dagdemir A, Karsli-Ceppioglu S, et al. Epigenetic modifications in prostate cancer. *Epigenomics* 2014;6:415–26.
3. Attard G, Parker C, Eeles RA, et al. Prostate cancer. *Lancet* 2016;387:70–82.
4. The molecular taxonomy of primary prostate cancer. *Cell* 2015;163:1011–25.
5. Ferro M, Buonerba C, Terracciano D, et al. Biomarkers in localized prostate cancer. *Future Oncol* 2016;12:399–411.
6. Valdes-Mora F, Clark SJ. Prostate cancer epigenetic biomarkers: next-generation technologies. *Oncogene* 2015;34:1609–18.
7. Smits M, Mehra N, Sedelaar M, et al. Molecular biomarkers to guide precision medicine in localized prostate cancer. *Expert Rev Mol Diagn* 2017; 17:791–804.
8. Thiery JP, Acloque H, Huang RY, et al. Epithelial-mesenchymal transitions in development and disease. *Cell* 2009;139:871–90.
9. Broster SA, Kyprianou N. Epithelial-mesenchymal transition in prostatic disease. *Future Oncol* 2015; 11:3197–206.
10. Kwok WK, Ling MT, Lee TW, et al. Up-regulation of TWIST in prostate cancer and its implication as a therapeutic target. *Cancer Res* 2005;65:5153–62.
11. Mani SA, Guo W, Liao MJ, et al. The epithelial-mesenchymal transition generates cells with properties of stem cells. *Cell* 2008;133:704–15.
12. Kong D, Banerjee S, Ahmad A, et al. Epithelial to mesenchymal transition is mechanistically linked with stem cell signatures in prostate cancer cells. *PLoS One* 2010;5:e12445.
13. Zhang J, Liu WL, Tang DC, et al. Identification and characterization of a novel member of olfactomedin-related protein family, hGC-1, expressed during myeloid lineage development. *Gene* 2002;283:83–93.
14. Liu W, Rodgers GP. Olfactomedin 4 expression and functions in innate immunity, inflammation, and cancer. *Cancer Metastasis Rev* 2016;35:201–12.
15. Chen L, Li H, Liu W, et al. Olfactomedin 4 suppresses prostate cancer cell growth and metastasis via negative interaction with cathepsin D and SDF-1. *Carcinogenesis* 2011;32:986–94.
16. Liu W, Liu Y, Zhu J, et al. Reduced hGC-1 protein expression is associated with malignant progression of colon carcinoma. *Clin Cancer Res* 2008;14: 1041–9.
17. Liu W, Lee HW, Liu Y, et al. Olfactomedin 4 is a novel target gene of retinoic acids and 5-aza-2′-deoxycytidine involved in human myeloid leukemia cell growth, differentiation, and apoptosis. *Blood* 2010;116:4938–47.
18. Liao Y, Smyth GK, Shi W. The subread aligner: fast, accurate and scalable read mapping by seed-and-vote. *Nucleic Acids Res* 2013;41:e108.
19. Micci F, Panagopoulos I, Haugom L, et al. Genomic aberration patterns and expression profiles of squamous cell carcinomas of the vulva. *Genes Chromosomes Cancer* 2013;52:551–63.
20. Yamanoi K, Arai E, Tian Y, et al. Epigenetic clustering of gastric carcinomas based on DNA methylation profiles at the precancerous stage: its correlation with tumor aggressiveness and patient outcome. *Carcinogenesis* 2015;36:509–20.
21. Clemmensen SN, Glenthoj AJ, Heeboll S, et al. Plasma levels of OLFM4 in normals and patients with gastrointestinal cancer. *J Cell Mol Med* 2015; 19:2865–73.
22. Jang BG, Kim HS, Kim KJ, et al. Distribution of intestinal stem cell markers in colorectal precancerous lesions. *Histopathology* 2016;68:567–77.
23. Jang BG, Lee BL, Kim WH. Olfactomedin-related proteins 4 (OLFM4) expression is involved in early gastric carcinogenesis and of prognostic significance in advanced gastric cancer. *Virchows Arch* 2015;467:285–94.
24. Ran X, Xu X, Yang Y, et al. A quantitative proteomics study on olfactomedin 4 in the development of gastric cancer. *Int J Oncol* 2015;47:1932–44.
25. Uzozie AC, Selevsek N, Wahlander A, et al. Targeted proteomics for multiplexed verification of markers of colorectal tumorigenesis. *Mol Cell Proteomics* 2017;16:407–27.
26. Yang Q, Bavi P, Wang JY, et al. Immunoproteomic discovery of tumor tissue autoantigens identifies olfactomedin 4, CD11b, and integrin alpha-2 as markers of colorectal cancer with liver metastases. *J Proteomics* 2017;168:53–65.
27. Marimuthu A, Chavan S, Sathe G, et al. Identification of head and neck squamous cell carcinoma biomarker candidates through proteomic analysis of cancer cell secretome. *Biochim Biophys Acta* 2013;1834:2308–16.
28. Yu L, He M, Yang Z, et al. Olfactomedin 4 is a marker for progression of cervical neoplasia. *Int J Gynecol Cancer* 2011;21:367–72.
29. Su W, Luo L, Wu F, et al. Low expression of olfactomedin 4 correlates with poor prognosis in smoking patients with non-small cell lung cancer. *Hum Pathol* 2015;46:732–8.
30. Xiong B, Lei X, Zhang L, et al. The clinical significance and biological function of olfactomedin 4 in triple negative breast cancer. *Biomed Pharmacother* 2017;86:67–73.
31. Mayama A, Takagi K, Suzuki H, et al. OLFM4, LY6D and S100A7 as potent markers for distant metastasis in estrogen receptor-positive breast carcinoma. *Cancer Sci* 2018;109:3350–9.
32. Quesada-Calvo F, Massot C, Bertrand V, et al. OLFM4, KNG1 and Sec24C identified by proteomics and immunohistochemistry as potential markers of early colorectal cancer stages. *Clin Proteomics* 2017;14:9.
33. Li H, Rodriguez-Canales J, Liu W, et al. Deletion of the olfactomedin 4 gene is associated with progression of human prostate cancer. *Am J Pathol* 2013;183:1329–38.
34. Bello D, Webber MM, Kleinman HK, et al. Androgen responsive adult human prostatic epithelial cell lines immortalized by human papillomavirus 18. *Carcinogenesis* 1997;18:1215–23.
35. Erickson HS, Gillespie JW. Emmert-Buck MR tissue microdissection. *Methods Mol Biol* 2008;424: 433–48.
36. Liu W, Chen L, Zhu J, et al. The glycoprotein hGC-1 binds to cadherin and lectins. *Exp Cell Res* 2006;312:1785–97.
37. Lukacs RU, Goldstein AS, Lawson DA, et al. Isolation, cultivation and characterization of adult murine prostate stem cells. *Nat Protoc* 2010;5: 702–13.
38. Li H, Velasco-Miguel S, Vass WC, et al. Epidermal growth factor receptor signaling pathways are associated with tumorigenesis in the Nf1:p53 mouse tumor model. *Cancer Res* 2002;62:4507–13.
39. Li H, Gu Y, Miki J, et al. Malignant transformation of human benign prostate epithelial cells by high linear energy transfer alpha-particles. *Int J Oncol* 2007;31:537–44.
40. Chin KL, Aerbajinai W, Zhu J, et al. The regulation of OLFM4 expression in myeloid precursor cells relies on NF-kappaB transcription factor. *Br J Haematol* 2008;143:421–32.
41. Liu W, Li H, Hong SH, et al. Olfactomedin 4 deletion induces colon adenocarcinoma in Apc(Min/+) mice. *Oncogene* 2016;35:5237–47.
42. Taylor BS, Schultz N, Hieronymus H, et al. Integrative genomic profiling of human prostate cancer. *Cancer Cell* 2010;18:11–22.
43. Li H, Liu W, Chen W, et al. Olfactomedin 4 deficiency promotes prostate neoplastic progression and is associated with upregulation of the hedgehog-signaling pathway. *Sci Rep* 2015;5: 16974.
44. Massie CE, Mills IG. Lynch AG the importance of DNA methylation in prostate cancer development. *J Steroid Biochem Mol Biol* 2017;166:1–15.
45. Yoon HY, Kim SK, Kim YW, et al. Combined hypermethylation of APC and GSTP1 as a molecular marker for prostate cancer: quantitative pyrosequencing analysis. *J Biomol Screen* 2012;17: 987–92.
46. Kawamoto K, Okino ST, Place RF, et al. Epigenetic modifications of RASSF1A gene through chromatin remodeling in prostate cancer. *Clin Cancer Res* 2007;13:2541–8.
47. Li H, Zhou J, Miki J, et al. Telomerase-immortalized non-malignant human prostate epithelial cells retain the properties of multipotent stem cells. *Exp Cell Res* 2008;314:92–102.
48. Miki J, Furusato B, Li H, et al. Identification of putative stem cell markers, CD133 and CXCR4, in hTERT-immortalized primary nonmalignant and malignant tumor-derived human prostate epithelial cell lines and in prostate cancer specimens. *Cancer Res* 2007;67:3153–61.
49. Park KS, Kim KK, Piao ZH, et al. Olfactomedin 4 suppresses tumor growth and metastasis of mouse melanoma cells through downregulation of integrin and MMP genes. *Mol Cells* 2012;34: 555–61.
50. Liu W, Zhu J, Cao L, et al. Expression of hGC-1 is correlated with differentiation of gastric carcinoma. *Histopathology* 2007;51:157–65.
51. Zhao J, Shu P, Duan F, et al. Loss of OLFM4 promotes tumor migration through inducing interleukin-8 expression and predicts lymph node metastasis in early gastric cancer. *Oncogene* 2016; 5:e234.
52. Park IK, Qian D, Kiel M, et al. Bmi-1 is required for maintenance of adult self-renewing haematopoietic stem cells. *Nature* 2003;423: 302–5.